

UDC 548.73:541.49:546.48

TWO NEW CADMIUM(II) COORDINATION POLYMERS WITH
BIS(BENZIMIDAZOLE) LIGANDS

X.-B. Liu, Y.-Q. Zhao, W.-L. Liu, G.-H. Cui

College of Chemical Engineering, North China University of Science and Technology, Tangshan, Hebei, P.R. China
E-mail: tscghua@126.com

Received October, 19, 2015

Revised — December, 2, 2015

Two new cadmium(II) coordination polymers, $\{[\text{Cd}(\text{L1})(\text{tbta})] \cdot \text{H}_2\text{O}\}_n$ (**1**) and $[\text{Cd}(\text{L2})(\text{tbta})]_n$ (**2**) (L1 = 1,4-bis(5,6-dimethylbenzimidazol-1-ylmethyl)benzene, H₂tbta = tetrabromoterephthalic acid and L2 = 1,4-bis(2-methylbenzimidazol-1-ylmethyl)benzene) are obtained under hydrothermal conditions and structurally characterized by single crystal X-ray diffraction methods, IR spectroscopy, TGA and elemental analysis. The L1 and L2 ligands differ by subtle variation of substituents at semi-rigid bis(benzimidazole) backbones. Complex **1** features a 3D threefold interpenetrating **dia** array with a 4-connected 6^o topology. Complex **2** displays a 2D $\{4^4 \cdot 6^2\}$ **sql/Shubnikov** tetragonal plane network. Complexes **1** and **2** possess high thermal stabilities and promising fluorescence behavior in the solid state.

DOI: 10.15372/JSC20170415

Keywords: bis(benzimidazole), cadmium(II) coordination polymer, crystal structure, fluorescence.

INTRODUCTION

Metal-organic coordination polymers (MOCPs) exhibit enticing properties indicating diverse promising applications in fluorescence, magnetism, storage, gas adsorption, ion exchange, and catalysis [1—4]. In order to gain the aesthetics of their molecular structures and topologies, we need continuous inspiration and additional exploratory synthetic efforts. Generally, these coordination frameworks are greatly influenced by metal ions, organic ligands, chosen solvent system, pH value and non-covalent interactions such as hydrogen-bonding and π — π interactions. Especially, judicious design of organic ligands is of pivotal importance [5—7]. In recent years, semi-rigid bis(benzimidazole) derivatives have attracted much interest as N-containing ligands for the construction of versatile coordination polymers [8—11]. The flexible nature of —(CH₂—C₆H₄—CH₂)— spacers allows these ligands to bend and rotate when coordinated to metal centers, in order to conform to the coordination preferences of the metal [12—16]. On the other hand, as an important family of multidentate/polytopic O-donor ligands, organic dicarboxylates are excellent negatively charged building blocks, with versatile coordination modes as well as the remarkable robustness, ideal for constructing higher dimensional networks with valuable properties. The inert halogen substituents of terephthalic acid derivatives have an important steric effect on coordination and supramolecular architectures [17—20]. Furthermore, the employment of mixed N-donor ligands together with aromatic dicarboxylates can compensate charge balance, coordination deficiency and weakly interaction all at once, which further enriches the versatility of coordination complexes [21—23].

In order to illustrate the influence of subtle variation of the substituents in semi-rigid bis(benzimidazoles), we present here the synthesis, structure and characterization of two new Cd coordination

polymers $\{[\text{Cd}(\text{L1})(\text{tbta})] \cdot \text{H}_2\text{O}\}_n$ (**1**) and $[\text{Cd}(\text{L2})(\text{tbta})]_n$ (**2**) (L1 = 1,4-bis(5,6-dimethylbenzimidazol-1-ylmethyl)benzene, and L2 = 1,4-bis(2-methylbenzimidazol-1-ylmethyl)benzene, H_2tbta = tetrabromoterephthalic acid). The thermal stability and fluorescence properties of two complexes were investigated in detail.

EXPERIMENTAL

Materials and physical measurements. All the reagents and solvents were purchased from Sinopharm Chemical Reagent Co., Ltd. and used directly without further purification. The L1 and L2 ligands were synthesized according to the literature [24]. Elemental analyses for C, H, and N were obtained with a Perkin-Elmer 240C elemental analyzer. The IR spectra were recorded on an Avatar 360 (Nicolet) spectrophotometer using KBr pellets in the region of 4000–400 cm^{-1} . Thermogravimetric analyses were performed on a NETZSCH TG 209 thermal analyzer from room temperature to 800 °C with a heating rate of 10 °C·min⁻¹ under N₂ atmosphere. Fluorescence spectra of powdered solid samples were measured on a Hitachi F-7000 fluorescence spectrophotometer at room temperature.

Synthesis of $\{[\text{Cd}(\text{L1})(\text{tbta})] \cdot \text{H}_2\text{O}\}_n$ (1**).** A mixture of CdCl₂ (0.2 mmol, 46 mg), L1 (0.1 mmol, 39 mg), H₂tbta (0.2 mmol, 96 mg), and H₂O (10 ml) was sealed in a 25-ml Teflon-lined autoclave and heated at 140 °C for 3 days under autogenous pressure. Afterwards, the autoclave was cooled to room temperature at a rate of 10 °C/h, colorless block-shaped crystals of **1** were obtained in 37 % yield based on Cd. Anal. Calcd for C₃₄H₂₈Br₄CdN₄O₅ (M_r = 1004.64) (%): C 40.65, H 2.81, N 5.58 %. Found (%): C 39.61, H 2.95, N 5.49 %. IR (cm^{-1}): 3400 s, 1577 s, 1421 m, 1332 s, 1303 m, 1216 s, 839 m, 695 w, 576 w, 526 w.

Synthesis of $[\text{Cd}(\text{L2})(\text{tbta})]_n$ (2**).** The synthetic procedure of **2** was analogous to that of **1**, except that L1 was used instead of L2 (0.2 mmol, 74 mg). Colorless block-shaped crystals of **2** were obtained. Yield: 28 % based on Cd. Anal. Calcd for C₃₂H₂₂Br₄CdN₄O₄ (M_r = 958.58) (%): C 40.10, H 2.31, N 5.84 %. Found (%): C 40.22, H 2.46, N 5.58 %. IR (cm^{-1}): 1615 s, 1512 m, 1460 w, 1324 s, 1299 s, 743 s, 575m, 529 m.

X-ray crystallography. X-ray single-crystal diffraction data for **1** were collected on an Agilent Technology SuperNova Atlas Dual diffractometer with a Cu microfocus source and focusing multi-layer optics ($\lambda = 1.54184$). The crystallographic data for **2** were collected on an Agilent Technology SuperNova Atlas Dual diffractometer with graphite monochromated MoK α radiation ($\lambda = 0.71073$ Å) by using a ω scan mode. Absorption corrections were applied with CrysAlis Pro software [25]. The structures were solved by direct methods with SHELXS-97 program [26] and refined with SHELXL-97 by full-matrix least squares fitting on F^2 [27]. All non-hydrogen atoms were refined anisotropically. In **1**, one water molecule is disordered and the structure was refined by the SQUEEZE routine of the PLATON program [28]. The detailed crystallographic information is summarized in Table 1. Selected bond lengths and angles for **1** and **2** are listed in Table 2. CCDC 1427917-1427918 contains the supplementary crystallographic data. These data can be obtained from the Cambridge Crystallographic Data Centre, 12 Union Road, Cambridge CB2 1EZ, UK; Fax: +44-1223-336033; E-mail: deposit@ccdc.cam.ac.uk.

RESULTS AND DISCUSSION

Crystal structure of $\{[\text{Cd}(\text{L1})(\text{tbta})] \cdot \text{H}_2\text{O}\}_n$ (1**).** Single crystal X-ray diffraction analysis reveals that **1** crystallizes in the monoclinic space group $C2/c$. The asymmetric unit of **1** consists of one independent Cd²⁺ ion, one L1 ligand, and two halves of tbta²⁻ ligands. As shown in Fig. 1, *a*, the Cd(II) center is five-coordinated by two nitrogen atom donors (N1, N3A) from two distinguish L1 ligands (symmetry code A: $-x+1/2, y-1/2, -z+3/2$) and three oxygen atom donors (O1, O2, O4) from two separated tbta²⁻ ligands in a slightly distorted square pyramidal geometry with $\tau_5 = 0.36$ ($\tau_5 = (\beta - \alpha)/60$; α, β are the two largest basic angles, $\tau_5 = 1$ for an ideal trigonal bipyramid and $\tau_5 = 0$ for an ideal square pyramid) [29]. The Cd—O bond distances vary from 2.252(3) to 2.450(3) Å, and the Cd—N bond lengths are 2.214(3)—2.279(4) Å, which is comparable to those observed elsewhere [30].

Table 1

Crystal data and structure refinements for complexes **1** and **2**

Compounds	1	2
Empirical formula	C ₃₄ H ₂₈ Br ₄ CdN ₄ O ₅	C ₃₂ H ₂₂ Br ₄ CdN ₄ O ₄
Formula weight	938.95	958.58
T, K	293(2)	293(2)
Wavelength, Å	1.54184	0.71073
Wavelength, Å; space group	Monoclinic; C2/c	Monoclinic; P2 ₁ /n
a, b, c, Å; β, deg.	37.2008(8), 19.1463(5), 10.0758(2); 96.059(2)	13.2282(3), 17.8369(3), 13.2974(3); 95.851(2)
V, Å ³	7136.5(3)	3121.18(11)
Z	8	4
D _{calc} , g/cm ³	1.870	2.040
Absorption coefficient, mm ⁻¹	10.536	5.866
F(000)	3904	1848
Crystal size, mm	0.22×0.20×0.19	0.20×0.19×0.17
θ range, deg.	4.26 to 67.07	2.56 to 26.37
h, k, l range	-26 ≤ h ≤ 44, -22 ≤ k ≤ 22; -12 ≤ l ≤ 11	-13 ≤ h ≤ 16, -16 ≤ k ≤ 22, -16 ≤ l ≤ 16
Reflections collected / unique	32243 / 6356	26248 / 6379
Max. and min. transmission	0.2208 and 0.1236	0.4038 and 0.3343
Refinement method	Full-matrix least-squares on F ²	Full-matrix least-squares on F ²
Independent reflections (R _{int})	6356 / 0.0720	6379 / 0.0545
Data / restraint / parameters	6356 / 0 / 428	6379 / 0 / 408
GOOF on F ²	0.902	1.095
Final R indices [I > 2σ(I)]	R1 = 0.0332, wR2 = 0.0825	R1 = 0.0389, wR2 = 0.0946
R indices (all data)	R1 = 0.0435, wR2 = 0.0884	R1 = 0.0610, wR2 = 0.1239
Residual peak and hole., e/Å ³	0.876, -0.750	1.443 and -1.373

Table 2

Selected bond lengths (Å) and angles (deg.) for complexes **1** and **2**

Parameter	Value	Parameter	Value	Parameter	Value
C ₃₄ H ₂₈ Br ₄ CdN ₄ O ₅ (1)					
Cd1—N1	2.214(3)	N1—Cd1—N3A	113.41(13)	N1—Cd1—O2	124.53(13)
Cd1—O2	2.252(3)	O2—Cd1—N3A	113.47(13)	O2—Cd1—O1	55.98(10)
Cd1—N3A	2.279(4)	N1—Cd1—O4	116.01(12)	N3A—Cd1—O1	89.90(11)
Cd(1)—O(4)	2.289(3)	O2—Cd1—O4	96.15(12)	O4—Cd1—O1	146.42(11)
Cd1—O1	2.450(3)	N3A—Cd1—O4	84.75(12)	N1—Cd1—O1	96.54(12)
C ₃₂ H ₂₂ Br ₄ CdN ₄ O ₄ (2)					
Cd1—N1	1.987(3)	N1—Cd1—O3B	120.10(15)	N1—Cd1—N4A	127.15(15)
Cd1—N4A	1.946(3)	N4A—Cd1—O1	107.12(15)	N4A—Cd1—O3B	101.02(15)
Cd1—O3B	2.227(4)	O3B—Cd1—O1	85.94(14)	N1—Cd1—O1	107.46(15)
Cd1—O1	2.238(4)				

Symmetry codes for **1**: A $-x+1/2, y-1/2, -z+3/2$; for **2**: A $x, y, z-1$; B $x+1/2, -y+1/2, z-1/2$.

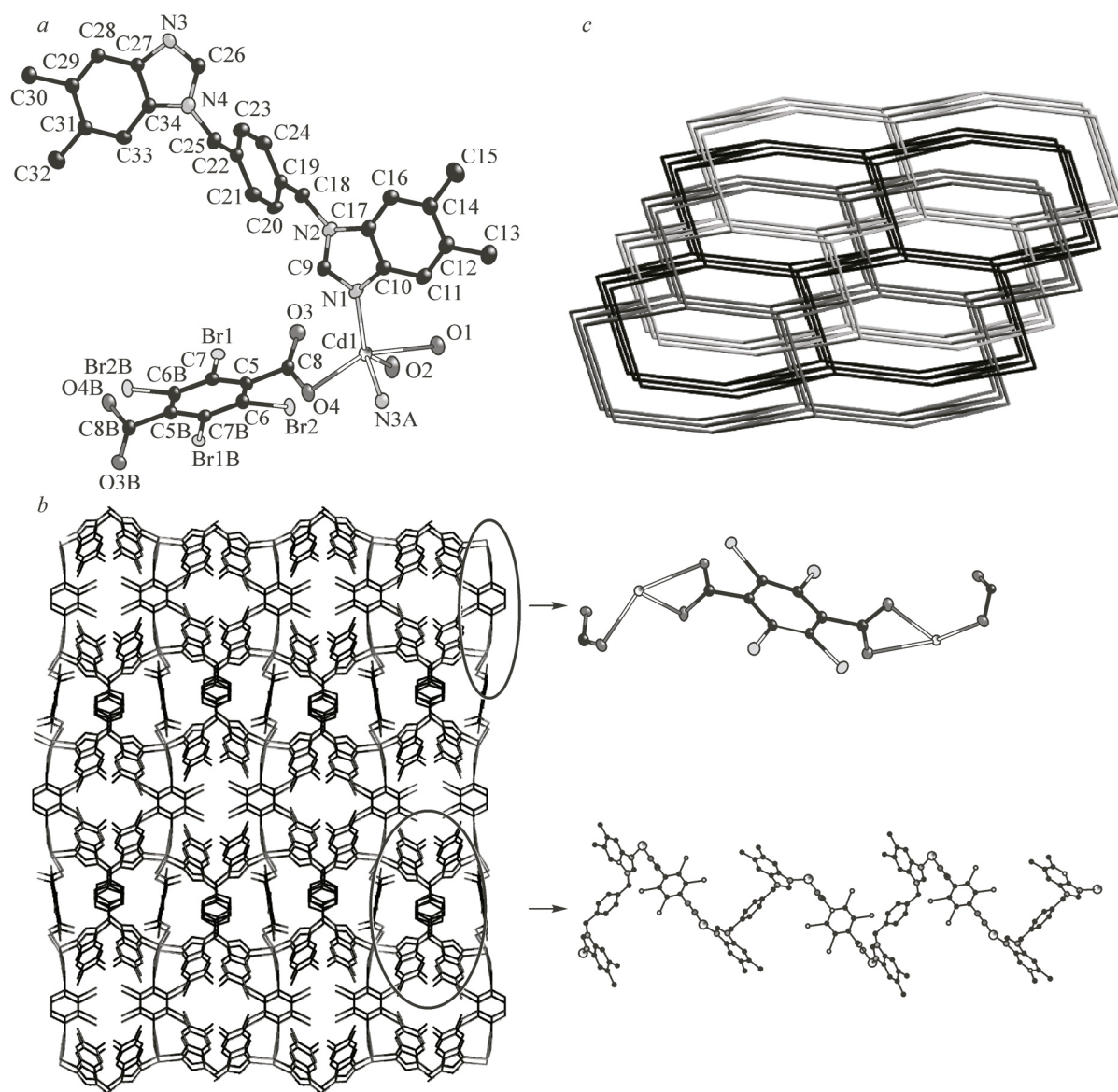


Fig. 1. Coordination environment around the Cd(II) ion in **1** at 30 % probability thermal ellipsoids, all hydrogen atoms were omitted for clarity (symmetry codes A: $-x+1/2, y-1/2, -z+3/2$; B: $-x+3/2, -y+3/2, -z$) (a); the single 3D **dia** net of **1** (b); the overall 3-fold interpenetrated construction and 6^6 topological representation (c)

In **1**, the 1D $[\text{Cd}(\text{tbta})]_n$ zigzag chain motif is formed by tbta^{2-} ligands with $\text{Cd}\cdots\text{Cd}$ distances of 11.335(5) Å and 11.028(5) Å. When coordinated to cadmium atoms, the tbta^{2-} ligands exhibit distinct coordination modes. One ligand adopts a bidentate chelating mode, and another is in a $\mu_2\text{-}\eta^1:\eta^1$ coordination mode. Further, the L1 ligands link the chains to generate an expanded diamond net (Fig. 1, b). The L1 ligand exhibits *anti*-conformation and acts as a μ_2 -bridging linker connecting adjacent Cd atoms with a $\text{Cd}\cdots\text{Cd}$ distance of 14.821(5) Å. The $\text{N}_{\text{donor}}\cdots\text{N}-\text{C}_{\text{sp}^3}\cdots\text{C}_{\text{sp}^3}$ torsion angles for the L1 ligands is 26.9(2)° and the dihedral angle between the mean planes of the two benzimidazole rings is 26.943(2)°. According to TOPOS 4.0 software [31], the potential voids of this 3D network are filled by two other mutually interpenetrating, independent equivalent frameworks, generating a 3-fold interpenetrating 3D **dia** architecture (Fig. 1, c). The three interpenetrated nets are related by a single translational vector (Class Ia) [32], with $Z_t = 3$ and $Z_n = 1$, where Z_t represents the number of interpenetrated nets related by translation, and Z_n denotes the number of interpenetrated nets related by crystal-

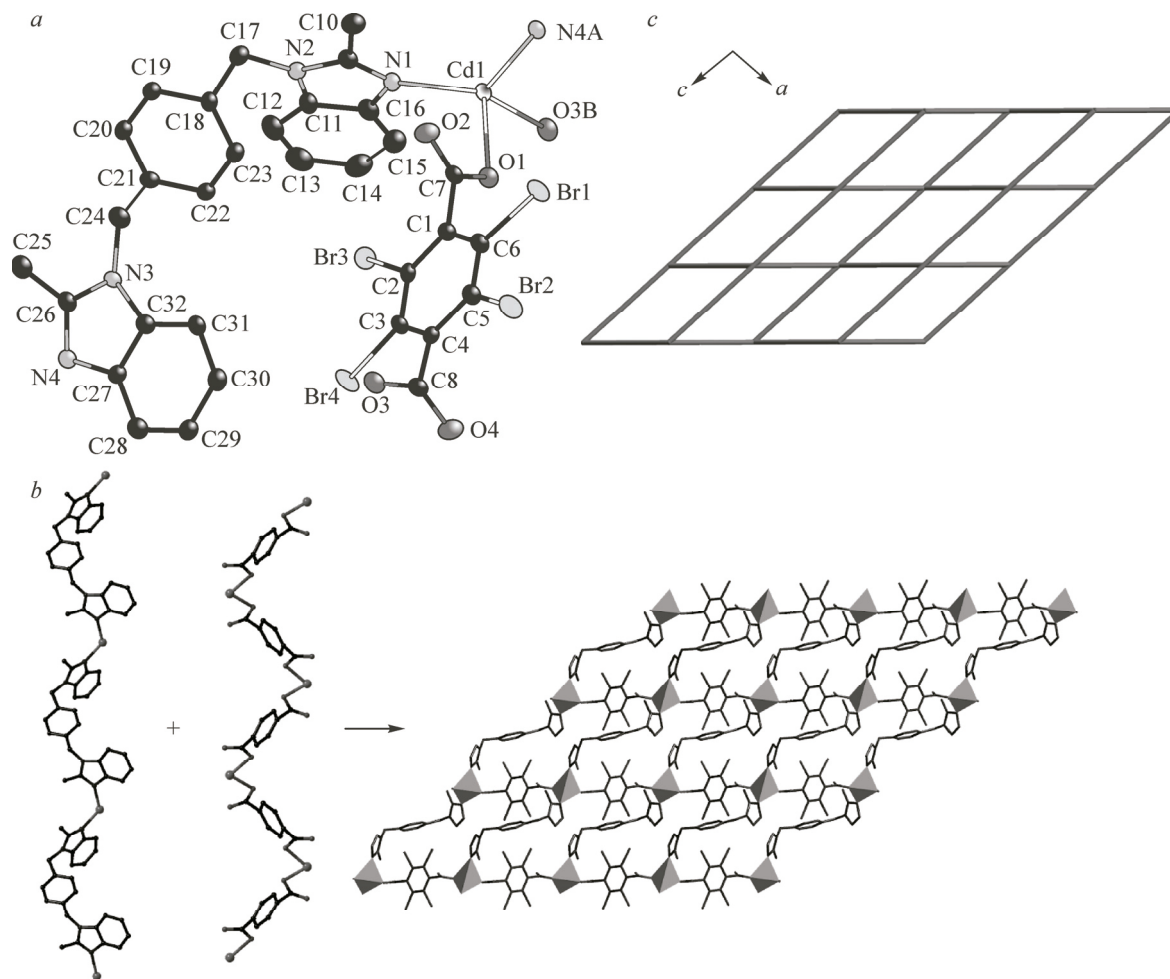
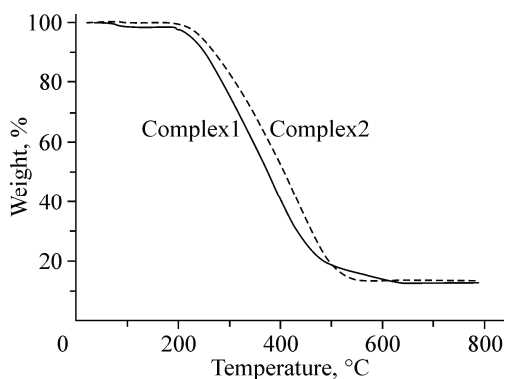


Fig. 2. Coordination environment around the Cd(II) ion in **2** at 30 % probability thermal ellipsoids, all hydrogen atoms were omitted for clarity (symmetry codes A: $x, y, z-1$; B: $x+1/2, -y+1/2, z-1/2$) (a); the 2D $\{4^4.6^2\}$ grid $[\text{Cd}(\text{L}2)(\text{tbta})]_n$ coordination polymer layer motif of **2**, all benzene rings of benzimidazole were omitted for clarity (b); the unimodal 4-connected 2D net in **2** (c)

lographic symmetry [33]. Intriguingly, void volume of 518.4 \AA^3 is still left after interpenetration, and the pore volume ratio was calculated to be 7.3 % by the PLATON program [34].

Crystal structure of $[\text{Cd}(\text{L}2)(\text{tbta})]_n$ (2**).** Complex **2** exhibits a 2D network and crystallizes in a monoclinic space group $P2_1/n$. The asymmetric unit of **2** consists of one independent Cd(II) atom, one L1 ligand, one tbta^{2-} ligand. As shown in Fig. 2, a, the Cd(II) center is four-coordinated displaying a slightly distorted $\{\text{CdO}_2\text{N}_2\}$ tetrahedral coordination sphere with the value of the $\tau_4 = 0.79$ [35]. The two carboxylate oxygen atoms O1, O3B (symmetry code B: $x+1/2, -y+1/2, z-1/2$) stemming from two different tbta^{2-} anions and one N1 atom of benzimidazole are located in the equatorial quasi-plane, whereas the apical position is occupied by N4A atom from L1 ligand (symmetry code A: $x, y, z-1$). The Cd—O/N bond distances varying from 2.227(4) Å to 2.238(4) Å and 2.196(4) Å to 2.215(4) Å, respectively, fall in their normal range [36].

The L2 ligands adopt a μ_2 -bridging coordination mode connecting the neighboring Cd(II) ions to construct a 1D $[\text{Cd}(\text{L}2)]_n$ linear chain with a dihedral angle of $81.9(2)^\circ$ between the mean planes of the two benzimidazole rings, and the $\text{N}_{\text{donor}} \cdots \text{N} - \text{C}_{\text{sp}^3} \cdots \text{C}_{\text{sp}^3}$ torsion angles $101.2(2)^\circ$ for the L2 ligands. The adjacent metal ions are connected by L2 ligands and tbta^{2-} anions in different directions into a 2D (4, 4) grid structure, in which the tbta^{2-} ligands adopt a bis-monodentate coordination mode (Fig. 2, b). The dimension of $\{\text{Cd}_4(\text{L}2)_2(\text{tbta})_2\}$ macrocycles formed by two L2 ligands, two tbta^{2-} ligands, and

Fig. 3. TG curves of **1** and **2**

four Cd(II) ions is $10.501(6) \times 11.322(6) \text{ \AA}$ as measured by through-space Cd \cdots Cd distances, with the Cd—Cd—Cd angles of $74.978(4)^\circ$ and $74.520(4)^\circ$. If each cadmium(II) center is considered as a four connected node and the tbta^{2-} , L2 ligands as linkers, coordination polymer **2** possesses a 2D four-connected **sql/Shubnikov** tetragonal planar structure with a point symbol of $\{4^4.6^2\}$ (Fig. 2, c).

Influence of the organic ligands on the structures.

In **1**, each N-donor ligand exhibits *anti*-conformation linking the neighboring Cd $^{2+}$ ions into *zigzag* chains, while in **2** each L2 ligand adopts *trans*-conformation mode, connecting the neighboring Cd $^{2+}$ ions into linear chains. The $\text{N}_{\text{donor}}-\text{N}-\text{C}_{\text{sp}^3}\cdots\text{C}_{\text{sp}^3}$ torsion angles are different in **1** and **2** ($26.9(2)^\circ$ for **1**, $101.2(2)^\circ$ for **2**), and result in different Cd \cdots Cd distances ($14.821(5) \text{ \AA}$ for **1**, $10.501(6)$ for **2**). Although both complexes contain the same dicarboxylate (tbta^{2-}) co-ligands, the coordination modes of the tbta^{2-} anions are distinct ($\mu_2-\eta^2:\eta^2$ and $\mu_2-\eta^1:\eta^1$ in **1**, $\mu_2-\eta^1:\eta^1$ in **2**). Complex **1** features a 3D threefold interpenetrating **dia** array with a 4-connected 6^6 topology, while in **2** the interlaced connection of the two kinds of 1D chains gives rise to **sql/Shubnikov** tetragonal plane network.

IR spectra. In the IR spectra of **1** and **2**, there are no strong absorption bands at around 1700 cm^{-1} demonstrating that all carboxylic groups of the H_2tbta ligands are deprotonated [37]. The characteristic asymmetric and symmetric vibration bands of the carboxylate groups appear at 1577 cm^{-1} , 1421 cm^{-1} , and 1332 cm^{-1} for **1** and 1615 cm^{-1} and 1324 cm^{-1} for **2**, with the $\nu_{\text{as}}(\text{COO})-\nu_{\text{s}}(\text{COO})$ separations indicating the presence of both monodentate (255 cm^{-1} for **1** and 203 cm^{-1} for **2**), and chelating (89 cm^{-1} for **2**) coordination modes of carboxylates [38, 39]. The strong broad band centered at around 3400 cm^{-1} in **1** refers to the O—H stretching vibration modes of water molecules. The bands at 1504 cm^{-1} for **1** and 1512 cm^{-1} for **2** can be assigned to $\nu_{\text{C}=\text{N}}$ of the N-heterocyclic rings of the benzimidazole-containing ligands.

Thermogravimetric analysis (TGA). To estimate the thermal stability of the two coordination polymers, TGA analyses were carried out. As shown in Fig. 3, in **1** the first weight loss of 1.7% (calcd.: 1.8%) starts at about 55°C and ends at 104°C , implying the removal of one water molecule. The second weight loss is observed in the range $208\text{--}603^\circ\text{C}$ (calcd.: 95.4%, found.: 95.6%), corresponding to the departure of the L1 and H_2tbta ligands. Complex **2** also shows two separate weight loss steps. The sharp weight loss occurs at about 218°C and ends at 569°C , implying the departure of the L2 and H_2tbta ligands. The total weight loss matches reasonably well with CdO as a putative remnant (for **1**: calcd.: 12.9%, found.: 12.7%; for **2**: calcd.: 13.1%, found.: 13.3%).

Fluorescent properties. Solid state fluorescence of complexes **1** and **2**, together with that of free N-donor ligands (L1 and L2), was studied at room temperature. The emission spectra are shown in Fig. 4. The free ligands display emission maxima at 316 nm and 309 nm , respectively ($\lambda_{\text{ex}} = 298 \text{ nm}$ for L1, and $\lambda_{\text{ex}} = 290 \text{ nm}$ for L2), which can be assigned to $\pi^* \rightarrow \pi$ transitions [40]. The complexes exhibit similar emission peaks with the maxima at 380 nm ($\lambda_{\text{ex}} = 298 \text{ nm}$) for **1** and 396 nm ($\lambda_{\text{ex}} = 290 \text{ nm}$) for **2**. Compared to the free ligands, the emission maxima of the complexes are red-shifted (by 64 nm for **1**, 87 nm for **2**). This suggests that fluorescence of the complexes originates mainly from the heterocyclic ligands and is to be assigned to the $\pi \rightarrow \pi^*$ transitions in the coordinated ligands, since the Cd $^{2+}$ ion is difficult to oxidize or reduce due to its very stable d^{10} configuration [41].

CONCLUSIONS

Two new Cd(II) coordination polymers based on tetrabromoterephthalate and semi-rigid bis(benzimidazole) co-ligands have been synthesized and characterized. The results of this study illustrate that the subtle variation of the substituent groups in semi-rigid bis(benzimidazole) and the coordination

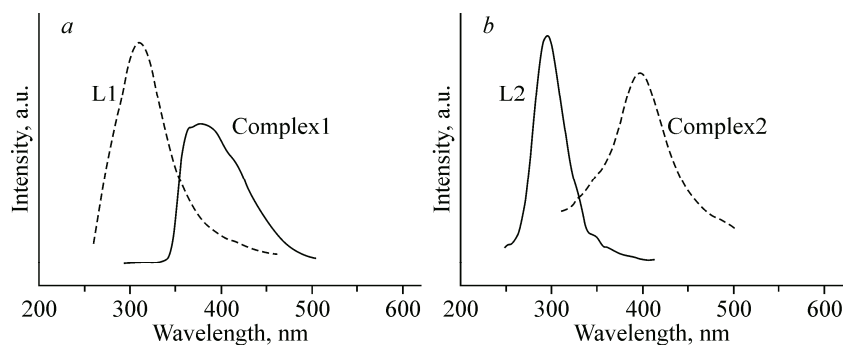


Fig. 4. The solid state fluorescence spectra of free ligand L1 and complex 1 (a) and the solid state fluorescence spectra of free ligand L2 and complex 2 (b)

modes of aromatic dicarboxylate anions can have great influence on the construction modes of resulting coordination polymers.

The project was supported by the National Natural Science Foundation of China (51474086), Natural Science Foundation-Steel and Iron Foundation of Hebei Province (B2015209299), the Graduate Student Innovation Fund of North China University of Science and Technology (2015S13) and the Hercules Foundation (project AUGÉ/11/029 "3D-SPACE: 3D Structural Platform Aiming for Chemical Excellence") and the Research Fund-Flanders (FWO) for funding.

REFERENCES.

- Alexandrov E.V., Blatov V.A., Kochetkov A.V., Proserpio D.M. // *CrystEngComm*. – 2011. – **13**. – P. 3947 – 3958.
- Wang X., Tian A.X., Wang X.L. // *RSC Adv*. – 2015. – **5**. – P. 41155 – 41168.
- Zhang H.M., Yang J., Liu Y.Y., Kang D.W., Ma J.F. // *CrystEngComm*. – 2015. – **17**. – P. 3181 – 3196.
- Du X., Wang Y.Y., Zhao Y.Q. et al. // *J. Struct. Chem.* – 2014. – **55**. – P. 734 – 738.
- Cui G.H., He C.H., Jiao C.H., Geng J.C., Blatov V.A. // *CrystEngComm*. – 2012. – **14**. – P. 4210 – 4216.
- Ma D.Y., Guo H.F., Qin L., Li Y., Ruan Q.T., Huang Y.W., Xu J. // *J. Chem. Crystallogr.* – 2014. – **44**. – P. 63 – 69.
- Xiao S.L., Zhao Y.Q., He C.H., Cui G.H. // *J. Coord. Chem.* – 2013. – **66**. – P. 89 – 97.
- Hao H.J., Liu F.J., Su H.F., Wang Z.H., Wang D.F., Huang R.B., Zheng L.S. // *CrystEngComm*. – 2012. – **14**. – P. 6726 – 6731.
- Liu Q.X., Zhao Z.X., Zhao X.J., Yao Z.Q., Li S.J., Wang X.G. // *Cryst. Growth Des.* – 2011. – **11**. – P. 4933 – 4942.
- Jiao C.H., Geng J.C., Geng C.H., Cui G.H. // *J. Mol. Struct.* – 2012. – **1020**. – P. 134 – 141.
- Hao J.M., Yu B.Y., Hecke K.V., Cui G.H. // *CrystEngComm*. – 2015. – **17**. – P. 2279 – 2293.
- Liu G.C., Huang J.J., Zhang J.W., Wang X.L., Lin H.Y. // *Transit. Met. Chem.* – 2013. – **38**. – P. 359 – 365.
- Xiao S.L., Qin L., He C.H., Du X., Cui G.H. // *J. Inorg. Organomet. Polym. Mater.* – 2013. – **23**. – P. 771 – 778.
- Wang X.X., Yu B.Y., Hecke K.V., Cui G.H. // *RSC Adv*. – 2014. – **4**. – P. 61281 – 61289.
- Guo Q.Q., Xu C.Y., Zhao D.D., Jia Y.Y., Wang X.J., Hou H.W., Fan Y.T. // *Z. Anorg. Allg. Chem.* – 2012. – **638**. – P. 868 – 873.
- Li C.P., Tian Y.L., Guo Y.M. // *Polyhedron*. – 2009. – **28**. – P. 505 – 510.
- Li C.P., Chen J., Du M. // *Polyhedron*. – 2010. – **29**. – P. 463 – 469.
- Li C.P., Chen J., Du M. // *CrystEngComm*. – 2010. – **12**. – P. 4392 – 4402.
- Du M., Li C.P., Liu C.S., Fang S.M. // *Coord. Chem. Rev.* – 2013. – **257**. – P. 1282 – 1305.
- Li H.H., Ma Y.J., Zhao Y.Q., Cui G.H. // *Transit. Met. Chem.* – 2014. – **40**. – P. 21 – 29.
- Xu C.Y., Li L.K., Wang Y.P., Guo Q.Q., Wang X.J., Hou H.W., Fan Y.T. // *Cryst. Growth Des.* – 2011. – **11**. – P. 4667 – 4675.
- Wang X.X., Zhang M.X., Yu B.Y., Hecke K.V., Cui G.H. // *Spectrochim. Acta, Part A*. – 2015. – **139**. – P. 442 – 448.
- Wang X.L., Hou L.L., Zhang J.W., Liu G.C., Lin H.Y. // *Polyhedron*. – 2013. – **61**. – P. 65 – 72.

24. *Aakeroy C.B., Desper J., Elisabeth E., Helfrich B.A., Levin B., Urbina J.F.* // *Z. Kristallogr.* – 2005. – **220**. – P. 325 – 332.
25. *Sheldrick G.M.* SADABS, Program for empirical absorption correction of area detector data, Univ. Göttingen, Germany, 1996.
26. *Sheldrick G.M.* SHELXS-97, University of Göttingen, Göttingen, Germany, 1997.
27. *Sheldrick G.M.* SHELXL-97, University of Göttingen, Göttingen, Germany, 1997.
28. *Spek A.L.* PLATON. A Multipurpose Crystallographic Tool, Utrecht University, Utrecht, 2000.
29. *Addison A.W., Rao T.N., Reedijk J. et al.* // *J. Chem. Soc., Dalton Trans.* – 1984. – **7**. – P. 1349 – 1356.
30. *Liu C., Cui G.H., Zou K.Y., Zhao J.L., Gou X.F., Li Z.X.* // *CrystEngComm.* – 2013. – **15**. – P. 324 – 331.
31. *Blatov V.A.* // *Struct. Chem.* – 2012. – **23**. – P. 955 – 963.
32. *Baburin I.A., Blatov V.A., Carlucci L., Ciani G., Proserpio D.M.* // *J. Solid State Chem.* – 2005. – **178**. – P. 2452 – 2474.
33. *Blatov V.A., Carlucci L., Ciani G., Proserpio D.M.* // *CrystEngComm.* – 2004. – **6**. – P. 378 – 395.
34. *Li J.R., Zhou H.C.* // *Angew. Chem. Int. Ed.* – 2009. – **48**. – P. 8465 – 8468.
35. *Yang L., Powell D.R., Houser R.P.* // *Dalton Trans.* – 2007. – **48**. – P. 955 – 964.
36. *He C.H., Jiao C.H., Cui G.H.* // *J. Struct. Chem.* – 2013. – **54**. – P. 168 – 172.
37. *Gu X.J., Dong F.X.* // *Cryst. Growth Des.* – 2006. – **6**. – P. 2551 – 2557.
38. *Deacon G.B., Phillips R.G.* // *Coord. Chem. Rev.* – 1980. – **33**. – P. 227 – 232.
39. *Teoh S.G., Ang S.H., Declercq J.P.* // *Polyhedron.* – 1997. – **16**. – P. 3729 – 3733.
40. *Zhang J.W., Gong C.H., Hou L.L., Tian A.X., Wang X.L.* // *J. Solid State Chem.* – 2013. – **205**. – P. 104 – 109.
41. *Geranmayeh S., Abbasi A., Skripkin M.Y., Badiei A.* // *Polyhedron.* – 2012. – **45**. – P. 204 – 212.